Surface core-level shifts of the polar semiconductor Cd(Zn)Te(100)

C. Heske, U. Winkler, G. Held, R. Fink, and E. Umbach
Experimentelle Physik II, Universität Würzburg, Am Hubland, D-97074 Würzburg, Germany

Ch. Jung, P. R. Bressler, and Ch. Hellwig
BESSY-GmbH, Lentzeallee 100, D-14195 Berlin, Germany
(Received 8 October 1996)

The termination of polar Cd(Zn)Te(100) surfaces is derived from an investigation of the surface core-level shifts in soft x-ray photoemission spectra of the Cd and Te $3d_{5/2}$ levels, leading to two groups of results. First, different surface preparations (i.e., sputter treatment and annealing under Cd flux, Te flux, or in ultrahigh vacuum) of Cd(Zn)Te single crystals result in clean, stoichiometric, and well-ordered surfaces. The influence of these preparations on reconstructions, surface core-level shifts, and in particular on the surface termination is demonstrated, deducing adequate conditions for a deliberate choice of the terminating atomic species. Second, the derived surface core-level shifts are discussed in view of photoelectron diffraction effects upon the variation of the detection angle and the photon energy of the synchrotron radiation, as well as in view of theoretical and experimental results for surface core-level shifts of different compound semiconductors. [S0163-1829(97)00828-X]

I. INTRODUCTION

The fabrication of electronic devices based on compound semiconductors with epitaxial methods such as molecular beam epitaxy (MBE) or atomic layer epitaxy (ALE) relies strongly on well-ordered, layered interfaces of different materials. In the case of II-VI semiconductors, in particular polar surfaces such as the zinc-blende (100) noncleavage planes are widely used to grow light-emitting diodes, lasers, and superlattices. For an optimized production of such devices a knowledge of the termination of these polar surfaces is of great importance. Moreover, any structural model of a polar compound-semiconductor surface has to explain the atomic configuration and thus the termination of both, reconstructed and unreconstructed, surfaces.

Several methods have been used to derive information about the termination of polar surfaces such as photoelectron diffraction,[1,2] chemical etching,[3] x-ray photoelectron intensity ratios,[3–7] electron diffraction,[3,8] scanning tunneling microscopy,[9] x-ray diffraction,[10] and photoemission surface core-level shifts of shallow core levels.[5,6] In many cases, however, a detailed interpretation and/or additional chemical knowledge are necessary to derive a conclusion about the surface termination.

In this paper we present results that demonstrate the straightforward determination of surface termination by photoemission surface core-level shifts (SCLS's) of relatively *deep* atomic levels such as the $3d$ levels of Cd and Te atoms in Cd(Zn)Te. The SCLS is defined as the shift in photoemission binding energy between the signal from bulk and that from surface atoms. Except for a Mg $K\alpha$ x-ray photoelectron spectroscopy (XPS) study on thin, strained CdTe layers,[7] almost all SCLS investigations of CdTe, both on cleavage and noncleavage planes, have been performed with synchrotron radiation using the Cd and Te $4d$ *shallow* core levels.[11–14] The spectral features of the Cd $4d$ levels are composed of the spin-orbit split bulk and surface components, superimposed by the Te $5s$ bulk and surface component, all of which show dispersion and have to be taken into account in band structure calculations.[15] Moreover, in the case of Cd(Zn)Te, the Zn $3d$ emission (spin-orbit split and surface-shifted) has also to be considered. To avoid such a large number of independent components, we have employed the high resolution at relatively high photon energies of the PM5 (HE-PGM3) beamline[16,17] and the HIRES photoelectron spectrometer at the BESSY synchrotron source to investigate the Cd and Te $3d_{5/2}$ *deep* core levels at photon energies yielding maximum surface sensitivity. In contrast to the above mentioned $4d$ levels, the spin-orbit split $3d$ levels of Cd and Te are well separated. Thus, only two distinct peaks are observed if a SCLS is present. By assuming equal widths for the surface and bulk components, respectively, one arrives at a total of six independent fit parameters for the peaks and two parameters for the simultaneously subtracted linear background.

In order to identify a surface-shifted component, we have employed variations of photon energy and detection angle hence changing the inelastic mean free path and the surface sensitivity of the photoelectrons, respectively. We will demonstrate that, in both cases, photoelectron diffraction effects have to be taken into account, but can nevertheless be separated in order to give an unambiguous identification of surface core-level shifts.

II. EXPERIMENT

Commercial, (100)-oriented Cd(Zn)Te single crystals with a nominal Zn content of 4% were chosen, since they are commonly used as a substrate for MBE/ALE purposes.[18] Due to the increased conductivity by Zn ''doping,'' no charging compensation had to be applied during our measurements. In order to derive an unambiguous interpretation of the surface termination, the samples were investigated at room temperature after different surface preparation treat-

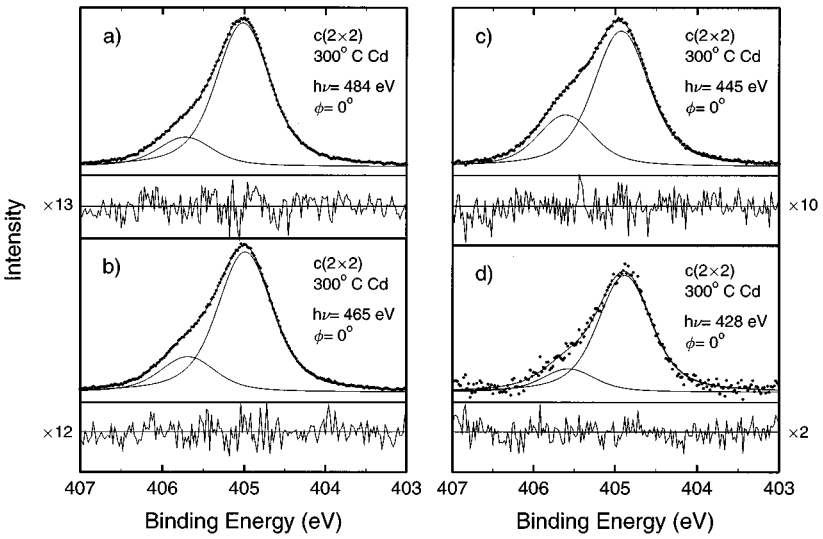

FIG. 1. Photoemission spectra of the Cd $3d_{5/2}$ core level for the $c(2\times2)$-reconstructed Cd(Zn)Te(100) surface. Spectra (a)–(d) show measurements for decreasing photon energy at normal emission ($\phi = 0°$). The surface-shifted component at higher binding energy has a maximum intensity at about $h\nu=445$ eV. Below each spectrum, the residual, i.e., the difference between the measurement and the Voigt-line shape fit, is shown. The magnification factors are given next to the baseline of the respective residual.

ments. An Ar^+-sputtering process at 1–2 keV was followed by annealing under Te flux (Te partial pressure 10^{-6} mbar), under Cd flux (Cd partial pressure 10^{-6} mbar), or under ultrahigh-vacuum (UHV) conditions at a base pressure of 2×10^{-10} mbar. Throughout the figures of this paper, an annealing step under, e.g., Te-flux at 300 °C will be denoted by ''300 °C Te.'' The detection angle ϕ is 0° for normal emission, i.e., the analyzer direction and the normal of the sample coincide. The surface quality and the reconstructions of the surface were monitored by low energy electron diffraction (LEED); the surface composition was investigated *in situ* by XPS using Mg $K\alpha$ radiation.

All binding energies are given with respect to the Fermi energy of a sputter-cleaned Au foil in electrical contact with the Cd(Zn)Te sample. Peak position variations within an energy range of 0.2 eV due to shifts in photon energy were detected during the course of our experiments. However, these variations do not affect the determination of surface core-level shifts presented in this paper.[19]

All present fits were performed by a χ^2-minimization procedure of symmetric Voigt line shapes. A linear background was simultaneously subtracted. It was assumed that the Gaussian and Lorentzian contributions to the Voigt profile are identical for surface and bulk components, leaving the peak positions, the relative heights, the respective full width at half maximum (FWHM), and the background as free parameters.

III. RESULTS

Throughout this paper, all data presented pertain to $Cd_{0.96}Zn_{0.04}Te(100)$ while results for the CdTe(100) surface have been published previously.[20,21] Both surfaces behave rather differently, as can be derived from their surface phase diagrams.[22] During the course of our experiments, we find a general enrichment of Zn for Cd(Zn)Te(100) within the photoemission information depth during annealing in UHV or under Cd flux as has first been reported by Wu *et al.*[23] for annealing in UHV. Sputter treatment reduces the Zn content at the surface substantially. In both cases [CdTe and Cd(Zn)Te], a spot profile analysis LEED investigation of the (100) surfaces determined the step height between surface terraces to be a double layer, so that a uniform termination is to be expected.[22]

Figure 1 shows the Cd $3d_{5/2}$ core level after a 300 °C annealing step under Cd flux, leading to a $c(2\times2)$ reconstruction. Spectra (a)–(d) were obtained at photon energies of 484 eV, 465 eV, 445 eV, and 428 eV. Below each spectrum the residual, i.e., the difference between the measurement and the fit, is depicted. The quality of the spectrum and its fit is characterized by a statistical distribution of the residual and by the magnification factor for each residual given at the baseline of the residual. A pronounced SCLS of about 0.7 eV towards higher binding energy is detected for all measurements, while the intensity of the surface-shifted component varies with photon energy and is maximized at $h\nu=$ 445 eV (i.e., at a kinetic energy of about 40 eV with respect to the Fermi energy) due to a minimization of the inelastic mean free path of the emitted photoelectrons. All fit parameters as well as the SCLS are summarized in Table I. For the $c(2\times2)$-reconstructed Cd(Zn)Te(100) surface, no surface shift of the Te $3d_{5/2}$ core level was found (not shown). Thus a Cd termination is deduced in agreement with results for CdTe(100) from XPS,[7] scanning tunneling microscopy (STM),[9] x-ray diffraction,[10] and synchrotron measurements.[20,21]

As mentioned, the relative intensity of the surface-shifted component at higher binding energy can be altered by varying the photon energy, thus influencing the inelastic mean free path of the emitted photoelectrons. Determining the ratio between the peak areas of the surface and bulk component, one derives the data points depicted as full circles in Fig. 2 (the solid line is intended as a guide to the eye). The bulk-to-surface peak area ratio is minimized (i.e., the surface sensitivity is maximized) at a kinetic energy of about 40 eV with respect to the Fermi energy (approximately 35 eV with respect to the vacuum level), while for smaller and higher kinetic energies the relative surface contribution is reduced. Plotted on a double-logarithmic scale, the resulting curve can be well compared to the dependence of the attenuation length on the emitted electron energy given by Seah and Dench[24] and more recently by Powell[25] and Gries.[26] Thus, the variation of photon energy can be easily used to identify surface-shifted spectral components.

TABLE I. Fit parameters and results for the SCLS's of Figs. 1, 3, 5, and 6. Also given are the Mg $K\alpha$-derived photoemission peak area ratios Cd/Te and Zn/(Cd+Te) of Cd $3d_{3/2}$, Te $3d_{3/2}$, and Zn $3p_{3/2}$ levels. For the Zn/(Cd+Te) ratio, the Cd $3d_{3/2}$ peak area has been multiplied by 2 in order to give equal weight to variations in the Cd- and Te-peak areas (for explanation, see text). The investigated surfaces are chronologically ordered from top to bottom (# denotes ± 0.1 eV).

Fig.	Element	Preparation	ϕ	$h\nu$ eV	SCLS's ± 0.05 eV eV	Gauss width ± 0.05 eV eV	Lorentz width ± 0.05 eV eV	Mg $K\alpha$ XPS I(Cd $3d_{3/2}$) / I(Te $3d_{3/2}$)	Mg $K\alpha$ XPS I(Zn $2p_{3/2}$) / $(2I_{Cd}+I_{Te})$
1(a)	Cd	300 °C Cd-$c(2\times2)$	0°	484	0.70	0.55	0.38		
1(b)	Cd	300 °C Cd-$c(2\times2)$	0°	465	0.70	0.56	0.39		
1(c)	Cd	300 °C Cd-$c(2\times2)$	0°	445	0.68	0.57	0.39		
1(d)	Cd	300 °C Cd-$c(2\times2)$	0°	428	0.69#	0.54#	0.38#		
3(a)	Cd	250 °C Cd-(1×1)	0°	444	0.66	0.56	0.38	0.53	0.17
3(b)	Cd	250 °C Cd-(1×1)	30°	444	0.65	0.59	0.36		
5(b)	Cd	350 °C UHV-(2×1)	0°	444	0.69	0.41	0.43	0.49	0.43
5(c)	Cd	350 °C UHV-(1×1)	0°	444	0.66	0.43	0.41	0.44	0.79
6(b)	Cd	350 °C Te-(2×1)	0°	444	0.66	0.39	0.43	0.40	1.63
6(g)	Te	300 °C Te-(2×1)*	0°	613	0.93	0.82	0.52	0.47	0.31
6(d)	Cd	+350 °C UHV-(2×1)*	30°	444	0.66	0.46	0.41	0.48	0.61

Such an identification is supported by a variation of the detection angle, as shown by the open squares in Fig. 2 (derived from the photoemission spectra to be presented in Fig. 3). In this case of a nominally unreconstructed (1×1) surface [showing a (1×1)-LEED pattern], the relative Cd surface contribution at normal emission [open square, (1×1), $\Phi=0°$] can be enhanced by a variation of the detection angle, e.g., by 30° [open square, (1×1), $\Phi=30°$]. Note that the bulk/surface intensity ratio for the (1×1) surface at 0° is larger than for the $c(2\times2)$-reconstructed surface. This is related to a higher degree of structural imperfections in the (1×1) case and perhaps to a Zn surface enrichment by the various sputter/annealing cycles performed before (quantitative XPS data could not be obtained in this case). An increased Zn content in the terminating surface layer would, of course, reduce the amount of Cd surface atoms and hence the intensity of the surface-shifted component.

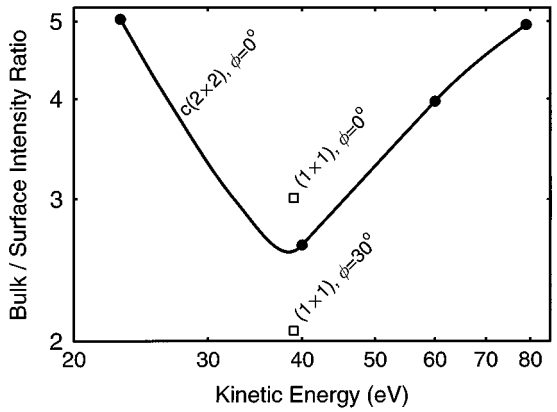

FIG. 2. Bulk-to-surface peak area ratio for the Cd $3d_{5/2}$ photoemission spectra of Fig. 1 (solid line) and Fig. 3 (open squares), depicting the variation of surface sensitivity with kinetic energy of the emitted electrons (i.e., with photon energy) and detection angle. The solid line is intended as a guide to the eye. The kinetic energy is referred to E_F.

As stated above, the open squares of Fig. 2 were derived from the data presented in Fig. 3 for the unreconstructed surface. Here, the Cd signal shows a pronounced shoulder [Fig. 3(a),(b)], while the Te signal (c) can be readily accounted for by a single Voigt-profile. Again, this leads to the interpretation of a Cd-terminated surface, as expected from the annealing procedure at 250 °C under Cd flux. The SCLS for the (1×1) structure is only slightly smaller than that derived for the $c(2\times2)$ reconstruction (see Table I).

As demonstrated in conjunction with Fig. 2, an identification of surface-shifted components can be easily accomplished by variation of the detection angle and/or by variation of the kinetic energy of the photoelectrons. This statement, however, has also to be viewed in the context of photoelectron diffraction (PED) effects. As shown in Fig. 4, the $c(2\times2)$ Cd-terminated surface shows pronounced diffraction effects for low kinetic energies upon variation of both, the photon energy and the detection angle, for the integrated Te $3d_{5/2}$ peak area, although the angular resolution was relatively poor ($\pm 10°$). While the Te emission undergoes significant changes of the emitted intensity, the Cd $3d_{5/2}$ signal hardly (if at all) oscillates with photon energy and is reduced only at lower kinetic energies, presumably due to a decrease of the photoemission cross section. Also, no PED effects can be detected by angular variation (not shown).

A quantum-mechanical calculation[27] based on tabulated muffin-tin local-density approximation (LDA) potentials for Cd (Ref. 28) reveals a preference of (single) forward scattering above a kinetic energy of about 35 eV relative to the ''muffin tin zero'' which, for semiconductors, can be set approximately equal to the Fermi level. Below 35 eV, the (single) backscattering channel becomes dominant. The ratio of backscattering to forward scattering intensity at a given

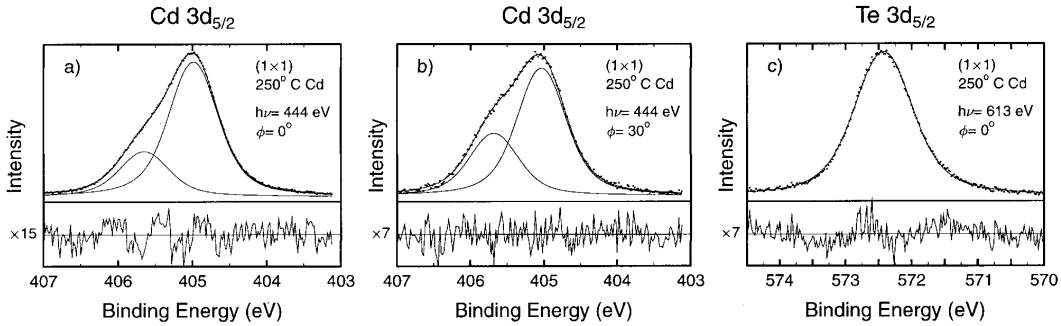

FIG. 3. Photoemission spectra of the Cd $3d_{5/2}$ (a, b) and the Te $3d_{5/2}$ core levels (c) of the (1×1)-unreconstructed Cd(Zn)Te(100) surface. The surface-shifted component of the Cd signal at normal emission (a) is significantly increased at $\phi=30°$ (b); no SCLS is detected for the Te signal (c).

electron energy ranges from 11 (at 20 eV) to 0.4 (at 60 eV). Consequently, a detailed investigation of the PED effects in the kinetic energy regime employed for the SCLS measurements will have to take both scattering paths (as well as multiple scattering) into account. While, in our case, significant PED effects can be detected, a combination of photon energy variation and changes in detection angle can be considered as a viable qualitative method to identify surface-shifted components of photoemission peaks.

A detailed quantitative analysis of the SCLS spectra, however, has to be performed with great care. In the first approximation, for instance, a Te SCLS towards higher binding energy would, according to Fig. 4 (Te 0°), result in a diminished surface component for kinetic energies between 20 and 30 eV, while the surface contribution would be overestimated in the 30–40 eV range. Note that the evaluation of Fig. 2 is nevertheless valid: in the case of a Cd SCLS the PED spectrum in Fig. 4 (Cd 0°) shows an almost linear behavior up to approximately 60 eV, thus diminishing the surface component by an equal amount for spectra 1(b)–(d). For higher kinetic energies, the intensity is constant (Fig. 4), so that in this case the surface component is determined correctly, while the first three data points in Fig. 2 (i.e., $E_{\mathrm{kin}}=23$, 40, and 60 eV) should be corrected only slightly towards lower bulk/surface intensity ratios.

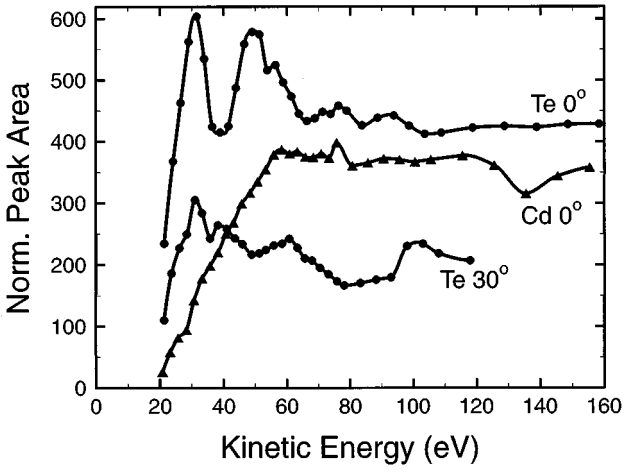

FIG. 4. Normalized integrated peak areas of the Cd and Te $3d_{5/2}$ photoemission peaks as a function of kinetic energy of the photoemitted electrons at normal emission (0°) and for a detection angle of 30° (Te 30°). Pronounced photoelectron diffraction effects are found for Te in the low kinetic energy regime.

The influence of a conventional sputter/annealing cycle in UHV on the SCLS is shown in Fig. 5. For solely sputtered surfaces (a, d) no SCLS can be detected for either the Cd or Te signal, but the line shape cannot be described satisfactorily by a symmetric Voigt profile, as can be seen from the residual. After sputter treatment, a short annealing of 20 min at 350°C in UHV leads to a long-range ordered (2×1) reconstruction with sharp LEED spots (b, e). After further annealing (4 h), the order is significantly reduced and/or (1×1) domains occur (c, f). This is presumably due to an enhanced Zn content, as can be derived from the last column in Table I. In both cases, the surface is identified as being Cd terminated since no SCLS in the Te $3d_{5/2}$ spectra is detected. A Cd surface termination was also detected for annealing temperatures down to 250 °C. The SCLS for the well-ordered (2×1)-reconstructed surface is slightly larger than in the less well-ordered case. However, the difference is very small, so that only a minor influence of the reconstruction on the SCLS can be concluded in this case (see Table I). The residual in Fig. 5(f) shows a slight deviation from the ideal statistical distribution, suggesting the presence of an additional Te minority species which, however, contributes less than 2.5%.

The results after annealing under Te-flux at various temperatures are shown in Fig. 6. An annealing temperature of 250 °C under Te flux is obviously low enough to allow an elemental Te multilayer (estimated thickness ≈35 Å) to be formed (a, e). No Cd is present within the information depth, while the Te line position significantly differs from the value for Te in Cd(Zn)Te. The LEED investigation reveals an ordered Te overlayer with a structure incompatible with Cd(Zn)Te. Again, the residual deviates somewhat from the ideal statistical distribution, suggesting the possible presence of more than one Te species (e.g., different Te states at the surface and within the Te layer). However, the deviation is again rather small (magnification ×8), so that a further deconvolution would lead to ambiguous results. In contrast to the formation of a Te layer at low (250 °C Te) annealing temperatures, the opposite effect is observed for annealing at 350 °C Te (b, f): a SCLS for the Cd signal and a single Voigt-profile for the Te peak suggest a Cd termination for the obtained (2×1) reconstruction. Apparently, the annealing

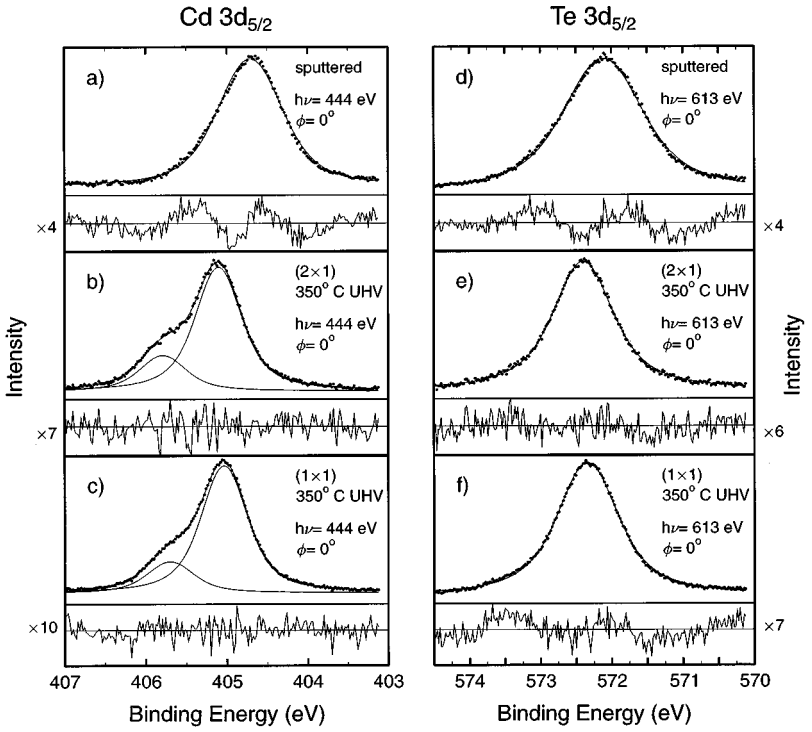

FIG. 5. Photoemission spectra of the Cd $3d_{5/2}$ (a)–(c) and Te $3d_{5/2}$ (d)–(f) core levels of Cd(Zn)Te(100) after sputter-treatment (a,d), of a strongly (2×1)-reconstructed surface after annealing at 350 °C in UHV (b,e), and of a (1×1)-unreconstructed surface with a ''weak'' (2×1) reconstruction [i.e., a minority of (2×1)-reconstructed areas] after further annealing at 350 °C (c,f).

temperature is too high to allow the Te atoms to form the terminating topmost layer.

Finally, annealing at 300°C Te leads to the desired effect of a Te termination: while no Cd SCLS is detected, the Te peak reveals a surface component shifted towards higher binding energy [Figs. 6(c) and (g)] with a surface-to-bulk peak area ratio of 1:8. Both, photon energy and detection angle variation, identify this peak as a surface component. Note that the line position of this surface component differs from the line position of the thick Te overlayer in (e) by 0.4 eV, ruling out a Te overlayer (i.e., Te atoms in a Te surrounding) at this annealing temperature, in accordance with the stoichiometry derived from Mg $K\alpha$ XPS. This surface is thus identified as being Te terminated, as is consistent with recent results from a Te-rich, (2×1)-reconstructed CdTe(100) surface derived from reflection high-energy electron diffraction (RHEED) and ALE.[29] The Te SCLS derived from the fit is significantly larger than any SCLS derived for Cd-terminated surfaces (see Table I), which will be discussed below. A further 20 min annealing of this Te-terminated surface in UHV at 350 °C (d, h) reverses the termination again: a SCLS is detected for the Cd and not for the Te signal, similar to the results presented in Fig. 5 but for a different reconstruction.

An interesting feature, which has not yet been observed, occurs in the LEED structure of the Te-terminated surface: judging from the spot intensities and their sharpness, two different superstructures are superimposed. Intense and sharp spots can be identified with a (2×1) superstructure, while additional less intense and broader features can be accounted for by a $(\sqrt{13/2}\times\sqrt{5/2})R33.7°$ structure. This composite structure [denoted $(2\times1)^*$] remains after additional annealing at 350 °C in UHV. Since such a structure has not been observed for CdTe, we suggest a possible connection with the influence of the Zn content in Cd(Zn)Te: during annealing in 10^{-6} mbar Te, a second (perhaps ZnTe-) phase is probably formed, which is stable during further annealing in UHV.

The experimentally derived SCLS's from Figs. 1, 3, 5, and 6 are summarized in Table I. Here, the parameters of the Voigt fits are also shown, together with the resulting SCLS for the respective core levels. Note that the values of the Lorentzian contribution to the FWHM of the Cd peaks are all very similar (Cd: 0.4 ± 0.05 eV, Te: 0.52 ± 0.05 eV) and that the Cd and Te widths are larger than the results of Prince *et al.* for the $4d$ levels of the CdTe(110) surface [Te: 0.3 ± 0.1 eV, Cd: 0.25 ± 0.1 eV (Ref. 11)], as is consistent with theoretical predictions of atomic-level widths.[30] Experimental results for metallic Cd and Te yielded a Lorentzian linewidth for the $3d_{5/2}$ levels of 0.33 eV and 0.61 eV,[31] respectively, in fair agreement with our results. The values of the Gaussian contribution to the FWHM vary due to the dependence of the photon energy linewidth on the source size of the stored electron beam at BESSY.

For Cd $3d_{5/2}$ in the $c(2\times2)$-reconstructed surface we find a SCLS of 0.7 eV and a slightly smaller value for all other reconstructions. As mentioned above, the SCLS of Te $3d_{5/2}$ for the Te-terminated surface is significantly larger (0.9 eV), and the surface component is shifted towards *higher* binding energies, just as the Cd SCLS for the Cd-terminated surfaces. These values have to be compared with results previously published for the $4d$ levels of CdTe: for the (110) cleavage plane Prince *et al.* derive a SCLS for Cd and Te of 0.24 eV and -0.26 eV, respectively.[11] The Cd SCLS has been confirmed by Wall *et al.*[14] For the (100) surface, John *et al.* interpreted the Te $5s$ emission as a second Cd surface component and derive a Cd SCLS of about 0.6 eV and -0.8 eV, respectively.[12,13] For one MBE preparation at 250 °C, they observe a Te SCLS of 1.0 eV towards higher binding energies in addition to the Cd SCLS. Finally, Tatarenko *et al.*

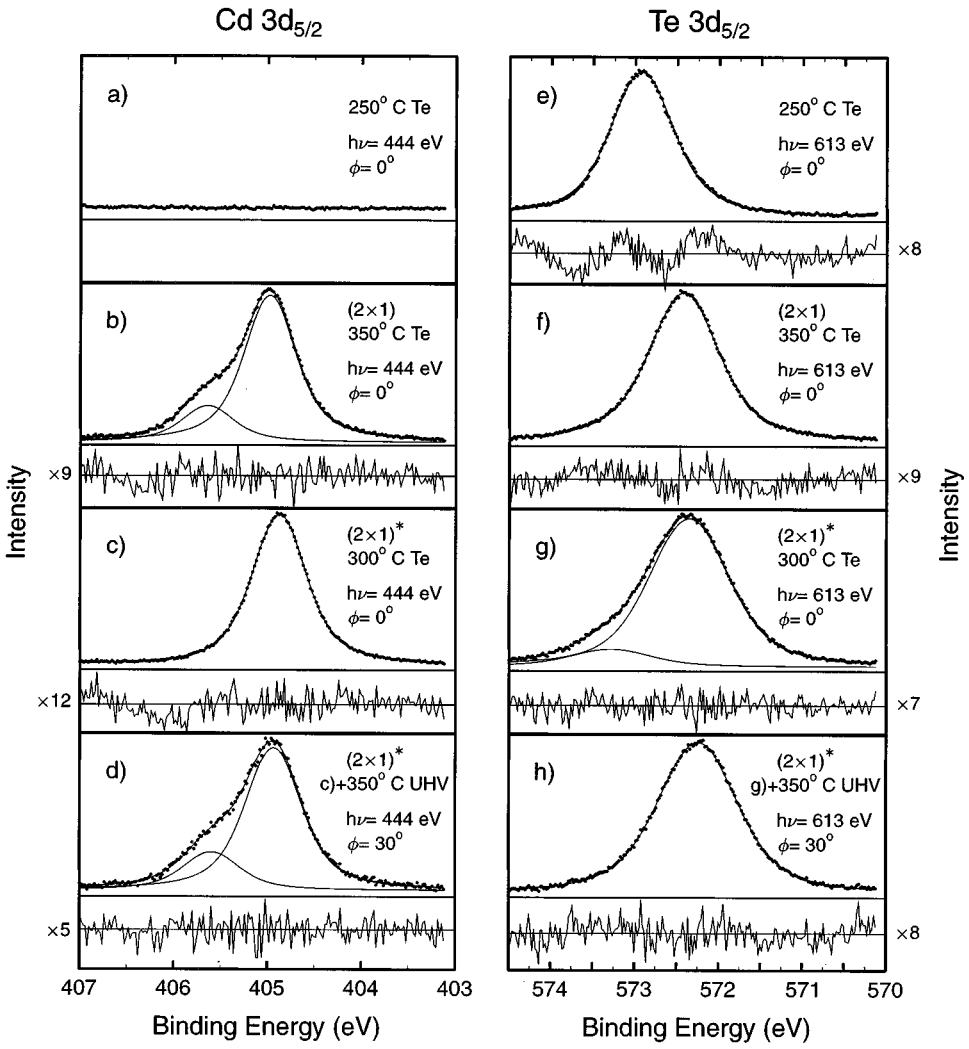

FIG. 6. Photoemission spectra of the Cd $3d_{5/2}$ (a–d) and Te $3d_{5/2}$ (e–h) core levels of Cd(Zn)Te(100) after annealing under Te flux: at 250 °C (a,e), at 350 °C (b,f), at 300 °C (c,g), and after a further UHV-annealing step at 350° (d,h). The (2×1)* LEED pattern is described in the text.

report a Mg $K\alpha$ XPS study of a thin, strained CdTe layer on ZnTe(100), for which a value of 0.4 eV was obtained for the Cd $3d_{3/2}$ SCLS with a pure Gaussian fit.[7] It is no surprise that results obtained for the (110) cleavage plane are different to those reported here for the polar (100) surface due to the different surface geometry and distribution of Cd and Te atoms. Moreover, we present Cd and Te SCLS results obtained for different surfaces (i.e., Cd or Te termination), while the SCLS results for the cleavage plane are determined from one single surface for both, Cd and Te. A more detailed discussion of the SCLS will be given in the following section. Comparing our results with those of the references for the (100) surface, we notice apparent similarities such as a Cd SCLS towards higher binding energy of at least 0.4 eV and also a Te SCLS towards higher binding energy. However, since the experimental and interpretational conditions differ significantly, a more detailed comparison seems difficult.

The evaluation of the Cd/Te and Zn/(Cd+Te) peak area ratios of the Cd $3d_{3/2}$, Te $3d_{3/2}$, and Zn $2p_{3/2}$ levels as derived by Mg $K\alpha$ XPS are also listed in Table I. A direct correlation between the Cd/Te ratios and the terminations [as has been assumed by Wu *et al.* for CdTe (Ref. 4)] appears questionable because of the above mentioned PED effects and is not possible in the case of Cd(Zn)Te, since the Zn content changes simultaneously. The Zn atoms are expected to occupy Cd sites and will thus change the intensity ratios, while the termination as derived from the Cd SCLS will be unaffected. Judging from the Zn/(Cd+Te) ratio, however, it is a general trend that in the course of our experiments the Zn content in the probing volume is—with one exception—significantly increased (note that Table I is chronologically ordered from top to bottom). For the determination of the Zn/(Cd+Te) ratio, the Cd-peak area has been multiplied by a factor of 2 in order to roughly eliminate the influence of different ionization cross sections, information depths, and analyzer transmissions. Thus, variations in both the Cd- and the Te-peak area are considered with equal weight. The general Zn enrichment at the surface is due to an interplay of sputter-induced Zn reduction and of Zn enhancement during annealing in UHV or 10^{-6} mbar Cd. The exception occurs for the Te-terminated surface [Figs. 6(c),(g)] and suggests that the sputter-induced reduction of the Zn content in the probing volume is *not* reversed by the annealing step under Te flux, in contrast to annealing in UHV or under Cd flux. At first sight, this finding is surprising, since the Zn atoms in Cd(Zn)Te are expected to occupy Cd sites. Thus, one would expect a decrease in Zn content after annealing under a Cd flux and a constant or an increased Zn content after annealing under a Te flux. However, the exponential dependence of

the photoemission signal on the depth of the emitting atom and on the inelastic mean free path leads to a decrease of the Zn signal for a Te-terminated surface (since Zn atoms are not allowed in the topmost layer) as compared to a Cd-terminated surface (where some of the surface Cd atoms are replaced by Zn). Therefore, the exception to the general increase of Zn surface content is directly correlated to the surface termination by Te atoms.

IV. DISCUSSION

A detailed understanding of the sign and magnitude of the observed shifts requires a discussion of the origin of SCLS's in general. The SCLS's of transition and rare earth metals have been explained on the basis of a narrowing of the valence band due to the reduced coordination number of atoms on the surface.[32,33] For compound semiconductors separate contributions to the SCLS's are still under debate. As pointed out by Egelhoff, a core-level shift can be related to a change in the electronic density distribution, influencing both the initial and the final state of the photoemission process.[34] An altered electron density can, in turn, be thought of as a change in the Madelung potential between the bulk and the surface,[35] a charge transfer between anions and cations, which is different between bulk and surface atoms,[36] or a bulk-to-surface change in the screening of the photoemission core hole.[34] Also, hybridization effects,[37] relaxations, and reconstructions have to be taken into account.

In case of GaAs(110), Eastman *et al.* interpreted their SCLS results with a geometry-dependent initial-state charge transfer.[36] Mönch pointed out that these SCLS's can be accounted for solely on the basis of a change in Madelung potential, since the calculated charge transfer is the same in the bulk and at the surface.[38] Prince *et al.* have transferred these results to the (more ionic) CdTe(110) cleavage plane and argue that their SCLS's are significantly smaller than the values expected for a sole reduction in the Madelung potential at the surface, so that other effects have to be taken into consideration as well.[11] A similar effect is reported by Paolucci *et al.* for the highly ionic semiconductor PbS, for which no SCLS could be detected for natural crystals within an accuracy of ± 0.1 eV.[39] In this case the SCLS is apparently determined not only by the ionicity but also by other effects such as relaxation.[40]

For the CdTe(100) and even more for the Cd(Zn)Te(100) surface, a distinction of the origins of the SCLS seems very difficult. While a tight-binding calculation for relaxed (110) surfaces of III-V semiconductors[41] yields results in good agreement with experiments for InP,[42] no such calculations are known for the polar (100) surfaces of zinc-blende II-VI compound semiconductors. This is presumably due to the fact that the geometric structures of the reconstructed surfaces are currently just on the verge of clarification.

Several conclusions about the nature of the SCLS's, however, can be derived from our data: the SCLS for Cd- and Te-terminated Cd(Zn)Te(100) surfaces are large and both lead to a surface-shifted component with *higher* binding energy, in contrast to the results reported for the (110) cleavage plane. While different surface reconstructions of the Cd-terminated surfaces cannot be correlated to large changes in the SCLS, there is a pronounced difference for Cd- and Te-terminated surfaces (0.65–0.70 eV and 0.9 eV, respectively). These SCLS values are equal or considerably larger than those reported for CdTe in the publications mentioned above. However, in comparing the different mechanisms leading to such surface core-level shifts, we have to keep in mind that in case of the cleavage plane the SCLS results for Cd and Te were obtained from the same sample surface, while in our case, Cd and Te SCLS's pertain to geometrically and electronically different (100) surfaces. Thus, influences such as a change in Madelung potential between bulk and surface or a reduced screening of the photoemission core hole can be very different for the Cd and Te termination.

The question now to be answered is how different SCLS origins affect the sign of the shift for unreconstructed (i.e., layered) surfaces. A change between the Madelung potential acting upon bulk and surface atoms will lead to a Cd (Te) shift towards higher (lower) binding energy, irrespective of the surface orientation [i.e., (100) or (110)], since atoms of opposite charge are missing from the immediate surrounding of the emitting surface atom, in agreement with the SCLS interpretation for GaAs(110).[38] In case of a change in charge transfer between cation and anion due to a different local surrounding of surface atoms as compared to bulk atoms, a decrease in charge transfer is expected (reconstructions ignored). Thus, the surface peaks are shifted towards lower (higher) binding energy for Cd (Te), in accordance with the argument of Prince *et al.* that the SCLS of CdTe(110) has to be explained by an additional change in charge transfer, since the shift is too small to be accounted for only on the basis of Madelung effects.[11] Again, this finding is irrespective of the surface orientation. Finally, a change in final state screening of the photoemission core hole at the surface results in a SCLS towards higher binding energy for both Cd and Te atoms.

So far, we have neglected any influence of reconstructions or relaxations on the SCLS of Cd and Te. Moreover, polar surfaces are known to lead to a depolarization effect of the topmost layer because of the repulsive interaction between adjacent, equally oriented dipoles. Therefore both, the change in Madelung potential and the difference in charge transfer between cation and anion are influenced, and hence the analysis of our results becomes more complicated than in the simple discussion given above.

According to our results, both the Cd and the Te surface peaks are shifted towards higher binding energies. Since these shifts are rather large (and different for Cd and Te), it seems unlikely that the major contribution is due to a decrease in final state screening. Moreover, the detailed interpretation of our results can be different for both Cd and Te, terminations. In the case of Cd termination, the SCLS is probably due to a combination of several effects. We believe that the Madelung potential plays an important role due to the high ionicity of CdTe, even though depolarization is expected. In addition, changes in charge transfer and final state screening may contribute. Note that for Cd termination, almost no influence of different reconstructions on the SCLS has been observed. This is not surprising since the major contributions to the SCLS's are predominantly determined by the nearest-neighbor distances which generally are similar for different surface reconstructions.

In the case of a Te SCLS, we ascribe the large SCLS

towards higher binding energy primarily to the existence of the (2×1)* reconstruction. A geometric model for the Te-terminated (2×1) reconstruction of CdTe(100) has recently been proposed, which is based on the formation of Te trimers at the polar surface.[43] In this model, the considerations given above would be invalid for the topmost Te atom of the surface trimer, since it would acquire a somewhat positively charged nature (as opposed to the negatively charged character in CdTe) leading to a higher binding energy. Moreover, the Te SCLS would be ''Cd-like'' in the sense that an influence of the Madelung potential would lead to a Te SCLS shift towards higher binding energy, as observed. Also, a slight decrease in final state screening is compatible with the experimental results. Further support for the (2×1) trimer model is derived from the fact that the Te termination could only be achieved under special preparation conditions, and, furthermore, that the intensity of the surface-shifted component is rather small, in accordance with the idea that only the topmost Te atoms of the surface trimer contribute to the Te SCLS. Thus, our experimental results for the SCLS of both the Cd and Te $3d_{5/2}$, can be qualitatively understood within the framework of the present model, although a SCLS of both elements, Cd and Te, in the same direction appears surprising at first glance.

V. CONCLUSIONS

We have presented direct evidence for a straightforward determination of the Cd(Zn)Te(100)-terminating surface layer by photoemission surface core-level shifts. Due to the high resolution of the PM5 (HE-PGM3) monochromator even at high photon energies, the low-lying $3d_{5/2}$ orbitals of Cd and Te have been used for the SCLS determination, thus significantly reducing the number of fit parameters needed as compared to the $4d$ levels. The viability of detecting surface-shifted components by variation of photon energy and detection angle has been demonstrated and discussed.

Sputter-cleaned samples exhibit no distinct SCLS, while annealing steps in UHV or under Cd flux lead to Cd-terminated surfaces with various surface reconstructions. Annealing steps under Te flux lead to a Te termination only at appropriate temperatures; moreover, the Te termination is unstable against further annealing under UHV, after which a Cd-terminated surface is formed again. Various preparation techniques have thus proven their ability to produce clean, well-ordered, and stoichiometric surfaces of Cd(Zn)Te single crystals with a uniform surface termination. The ease and high quality of the presented surface preparation by sputter/annealing cycles may be of great importance for the epitaxial growth of semiconductor heterojunctions without the need of an additional epitaxial CdTe buffer layer as substrate material.

The sign and magnitude of the observed SCLS can be explained qualitatively on the basis of a dominant change in Madelung potential between surface and bulk atoms in the case of a Cd termination and a large influence of the observed reconstruction on the SCLS of the Te-terminated surface. Evidence for a geometric model of Te-trimer formation for the Te-terminated (2×1)-reconstructed CdTe(100) surface can be derived from our results of the Te surface core-level shift for (2×1)* Cd(Zn)Te.

ACKNOWLEDGMENTS

We would like to thank H. Neureiter, M. Sokolowski, F. von Ludowig, and S. Tatarenko for their help and useful discussions and the BESSY staff for technical support. Financial support by the Deutsche Forschungsgemeinschaft through SFB 410 is gratefully acknowledged.

[1] S. A. Chambers, Phys. Rev. B **42**, 10 865 (1990); J. Vac. Sci. Technol. A **8**, 2062 (1990).
[2] R. Duszak, S. Tatarenko, J. Cibert, K. Saminadayar, and C. Deshayes, J. Vac. Sci. Technol. A **9**, 3025 (1991).
[3] C. Hsu, S. Sivanathan, X. Chu, and J. P. Faurie, Appl. Phys. Lett. **48**, 908 (1986).
[4] Y. S. Wu, C. R. Becker, A. Waag, M. M. Kraus, R. N. Bicknell-Tassius, and G. Landwehr, Phys. Rev. B **44**, 8904 (1991).
[5] W. Chen, A. Kahn, P. Soukiassian, P. S. Mangat, J. Gaines, C. Ponzoni, and D. Olego, J. Vac. Sci. Technol. B **12**, 2639 (1994); Phys. Rev. B **49**, 10 790 (1994).
[6] P. John, T. Miller, and T.-C. Chiang, Phys. Rev. B **39**, 1730 (1989).
[7] S. Tatarenko, F. Bassani, J. C. Klein, K. Saminadayar, J. Cibert, and V. H. Etgens, J. Vac. Sci. Technol. A **12**, 140 (1994).
[8] S. Tatarenko, B. Daudin, D. Brun, V. H. Etgens, and M. B. Veron, Phys. Rev. B **50**, 18 479 (1994).
[9] L. Seehofer, G. Falkenberg, R. L. Johnson, V. H. Etgens, S. Tatarenko, D. Brun, and B. Daudin, Appl. Phys. Lett. **67**, 680 (1995).
[10] M. B. Veron, M. Sauvage-Simkin, V. H. Etgens, S. Tatarenko, H. A. Van der Vegt, and S. Ferrer, Appl. Phys. Lett. **67**, 3957 (1995).
[11] K. C. Prince, G. Paolucci, V. Cháb, M. Surman, and A. M. Bradshaw, Surf. Sci. **206**, L871 (1988).
[12] P. John, T. Miller, T. C. Hsieh, A. P. Shapiro, A. L. Wachs, and T.-C. Chiang, Phys. Rev. B **34**, 6704 (1986).
[13] P. John, F. M. Leibsle, T. Miller, T. C. Hsieh, and T.-C. Chiang, Superlattices Microstruct. **3**, 347 (1987).
[14] A. Wall, Y. Gao, A. Raisanen, A. Franciosi, and James R. Chelikowsky, Phys. Rev. B **43**, 4988 (1991).
[15] S. H. Wei and A. Zunger, Phys. Rev. B **37**, 8958 (1988).
[16] H. Petersen, C. Jung, C. Hellwig, W. B. Peatman, and W. Gudat, Rev. Sci. Instrum. **66**, 1 (1995).
[17] Ch. Jung, *Research at BESSY-A User's Handbook*, edited by Ch. Jung (BESSY, Berlin, 1995).
[18] E.g., Ref. 8 and Y. S. Wu, C. R. Becker, A. Waag, K. von Schierstedt, R. N. Bicknell-Tassius, and G. Landwehr, Appl. Phys. Lett. **62**, 1510 (1993).
[19] The PM5 (HE-PGM3) monochromator uses the stored electron beam of the BESSY storage ring directly as a photon source without a further entrance slit. Thus, variations in electron orbit position can lead to changes in photon energy between different storage ring injections, which have to be accounted for in separate calibration measurements. Since the measurement time for a SCLS spectrum is in the order of 2–3 h, we have aimed at

minimizing contamination effects from the residual gas by performing calibration measurements for only approximately every fifth injection, leading to an overall accuracy in the order of 0.2 eV.

[20] C. Heske, U. Winkler, R. Fink, E. Umbach, Ch. Jung, P. R. Bressler, and Ch. Hellwig, *The Physics of Semiconductors*, edited by M. Scheffler and R. Zimmermann (World Scientific, Singapore, 1996), p. 823.

[21] C. Heske, U. Winkler, H. Neureiter, M. Sokolowski, R. Fink, E. Umbach, Ch. Jung, and P. R. Bressler, Appl. Phys. Lett. **70**, 1022 (1997).

[22] H. Neureiter, S. Spranger, M. Sokolowski, and E. Umbach, Surf. Sci. (to be published).

[23] Y. S. Wu, C. R. Becker, A. Waag, R. N. Bicknell-Tassius, and G. Landwehr, Appl. Phys. Lett. **60**, 1878 (1992).

[24] M. P. Seah and W. A. Dench, Surf. Interface Anal. **1**, 2 (1979).

[25] C. J. Powell, Surf. Sci. **299/300**, 34 (1994), and references therein.

[26] W. H. Gries, Surf. Interface Anal. **24**, 38 (1996).

[27] A.R. Williams's phase shift program (19.10.1985) (unpublished).

[28] V. L. Moruzzi, J. F. Janak, and A. R. Williams, *Calculated Electronic Properties of Metals* (Pergamon Press, New York, 1978).

[29] B. Daudin, D. Brun-Le Cunff, and S. Tatarenko, Surf. Sci. **352-354**, 99 (1996).

[30] O. Keski-Rahkonen and M. O. Krause, At. Data Nucl. Data Tables **14**, 139 (1974).

[31] N. Mårtensson and R. Nyholm, Phys. Rev. B **24**, 7121 (1981).

[32] P. H. Citrin, G. K. Wertheim, and Y. Baer, Phys. Rev. Lett. **41**, 1425 (1978).

[33] D. E. Eastman, F. J. Himpsel, and J. F. van der Veen, J. Vac. Sci. Technol. **20**, 609 (1982).

[34] W. J. Egelhoff, Jr., Surf. Sci. Rep. **6**, 253 (1987).

[35] R. E. Watson, J. W. Davenport, M. L. Perlman, and T. K. Sham, Phys. Rev. B **24**, 1791 (1981).

[36] D. E. Eastman, T.-C. Chiang, P. Heimann, and F. J. Himpsel, Phys. Rev. Lett. **45**, 656 (1980).

[37] R. E. Watson and J. W. Davenport, Phys. Rev. B **27**, 6418 (1983).

[38] W. Mönch, Solid State Commun. **58**, 215 (1986).

[39] G. Paolucci and K. C. Prince, Phys. Rev. B **41**, 3851 (1990).

[40] G. Allan, Phys. Rev. B **43**, 9594 (1991).

[41] C. Priester, G. Allan, and M. Lannoo, Phys. Rev. Lett. **58**, 1989 (1987).

[42] T. Kendelewicz, P. H. Mahowald, K. A. Bertness, C. E. McCants, I. Lindau, and W. E. Spicer, Phys. Rev. B **36**, 6543 (1987).

[43] M. B. Veron, Ph.D. thesis, Université Pierre et Marie Curie-Paris VI, 1996.